



# Efficient Extraction and Characterization of Pectin from Pomelo Peel by Sequential Ultrasonic and Radio Frequency Treatment

Jin Wang<sup>1</sup> · Sicheng Du<sup>1</sup> · Hongyue Li<sup>1</sup> · Shaojin Wang<sup>1,2</sup> · Bo Ling<sup>1</sup>

Received: 18 March 2024 / Accepted: 23 July 2024

© The Author(s), under exclusive licence to Springer Science+Business Media, LLC, part of Springer Nature 2024

## Abstract

The aim of this study was to optimize sequential ultrasound-radio frequency–assisted extraction (URAE) of pectin from pomelo peel. Effects of sonication power and time, radio frequency (RF) heating temperature, and time on the pectin yield (PY) were evaluated. Based upon optimized URAE parameters, the yield, physicochemical, and structure properties of pectin recovered from sequential radio frequency-ultrasound–assisted extraction (RUAE), ultrasound-assisted extraction (UAE), and RF-assisted extraction (RFAE) were also compared. A maximal PY of  $28.36 \pm 0.85\%$  was attained at the optimized URAE conditions including solvent pH of 1.5 (citric acid), sonication at 183 W for 24 min, and RF heating at 87 °C for 23 min. Although all four samples had a high degree of esterification more than 50%, URAE was the lowest. No significant changes were observed in the types of monosaccharides among different samples. Furthermore, all four samples (6.6–10.3 mg GAE/g) showed significantly higher total phenolic content than those of commercial citrus pectin (1.2 mg GAE/g), and among them, RFAE was the highest with the best antioxidant capacity. The water and oil holding capacities of the four samples were between 3.5 to 4.0 and 2.6 to 3.0 g/g, respectively, but there was no significant difference ( $p > 0.05$ ) between each other. Structure properties indicated that there were no significant differences in the main chemical structures among the four pectin samples. Morphology analysis of URAE showed a more compact, smoother, and flatter surface than that of RUAE and RFAE. The results observed in this paper suggest that sequential URAE is an efficient strategy for the recovery of high-quality pectins.

**Keywords** Radio Frequency Heating · Physical Fields · Ultrasound-radio Frequency–assisted Extraction · Pectin · Physicochemical Properties

## Abbreviations

CE	Conventional extraction
DE	Degree of esterification
GaLA	Galacturonic acid
HMP	High methoxyl pectin
MW	Microwave
MWAE	Microwave-assisted extraction
PFAE	Physical field–assisted extraction
PP	Pomelo peel
PPP	Pomelo peel pectin

PPASM	Pomelo peel-acid solution mixture
PY	Pectin yield
RF	Radio frequency
RFAE	Radio frequency–assisted extraction
RUAE	Radio frequency-ultrasound–assisted extraction
UAE	Ultrasound-assisted extraction
UMAE	Ultrasound-microwave–assisted extraction
URAE	Ultrasound-radio frequency–assisted extraction
US	Ultrasound

✉ Bo Ling  
6lb6lb@nwsuaf.edu.cn

<sup>1</sup> College of Mechanical and Electronic Engineering, Northwest A&F University, Yangling 712100, Shaanxi, China

<sup>2</sup> Department of Biological Systems Engineering, Washington State University, 213 L.J. Smith Hall, Pullman, WA 99164-6120, USA

## Introduction

Pomelo is the largest and juiciest fruit of the citrus family, which is indigenous to Southeast Asia and is now one of the most widely cultivated and consumed citrus fruits all over the world (Tocmo et al., 2020). Pomelo peel (PP) makes up about 30% of the fresh fruit weight, and is a good source of pectin since the albedo part contains more than 20% of the pectin (Xiao et al.,

2021). Thus, extraction of PP pectin (PPP) is an important way for the valorization of pomelo processing by-products.

Pectin is a heteropolysaccharide abundant in the cell wall and middle lamella of terrestrial plants, mainly extracted from citrus peel and apple pomace, and widely used in the food, cosmetic, and pharmaceutical industries as a stabilizer, emulsifier, thickening, or gelling agent (Cui et al., 2021). Conventional extraction (CE) typically requires soaking raw materials in water acidified with strong mineral acids, and conductive heating, such as hot water, is the most used method to improve the hydrolysis and mass transfer. Although CE is a well-established industrial process, low pH, high temperature, and long treatment times are needed to obtain a desirable pectin yield (PY), resulting in obvious disadvantages, such as thermal de-polymerization, equipment corrosion, and environmental pollution.

In connection with the emerging concept of “green technology,” the introduction of physical field-assisted extraction (PFAE), such as ultrasound (US) and microwave (MW) for assisted pectin extraction, has attracted considerable attention due to their higher efficiency, eco-friendly, and better product quality (Ling et al., 2023). It is generally considered that the US-induced physical phenomena include fragmentation in cellular structure, localized erosion of plant matrix surface, pore formation in cell membranes, and shear stress or turbulence within the liquid, which are the major mechanisms for US-assisted extraction (UAE) (Gerschenson et al., 2021; Tao et al., 2022). Microwave-assisted extraction (MWAE) is a thermal-based method that directly heats the cell matrix, increasing intracellular pressure, causing the biomass cell wall rupture, and promoting solute release. Furthermore, it can increase the temperature of the solvent rapidly, resulting in a fast solute diffusion rate; thus, the mass transfer can be completed in several minutes (Tao et al., 2021).

More recently, radio frequency (RF) heating has also attracted some attentions in the pectin extraction (Gao et al., 2023b). RF energy is more suitable for heating bulk materials both due to its deeper penetration depth (i.e., 11 m at 27.12 MHz RF wave versus 0.12 m at 2450 MHz MW in free space) and simpler or more uniform electromagnetic field patterns (Gao et al., 2023a). RF heating has been used in protein modification (Liu et al., 2023), pasteurization (Muñoz et al., 2022), drying (Mahmood et al., 2023), and disinfestations (Li et al., 2022), etc. For the pectin extraction, it was first reported by Naik et al. (2020) from jackfruit peel. In another study, Zheng et al. (2021) optimized the RF-assisted extraction (RFAE) of apple pomace pectin.

Although different PFAE have been used for studying pectin recovery, it is unlikely that a single technique can simultaneously meet all requirements. Thus, multi-PFAE, such as manosonication (Hu et al., 2021), US-MW (Tien et al., 2022), and pulsed electric field-MW-assisted extraction (Lal et al., 2021), is also recommended due to their more effective

yield and better product quality. Among them, the sequential combination of UAE and MWAE is one of the most studied hybrid techniques, which can be performed via two individual reactors without the need to build a special device. For example, Gharibzahedi et al. (2019b) optimized the sequential ultrasound-microwave-assisted extraction (UMAE) of pectin from fig skin, and the results showed that the extracted pectin with high lightness contained considerable amounts of uronic acid and neutral monosaccharides. Besides, Sengar et al. (2020) reported that there was very less difference in the yield between sequential UMAE and sole MWAE of pectin from tomato peel, but the degree of esterification (DE) was higher and color was better for UMAE.

Similar to MWAE, RFAE also is a thermal-based method with better heating uniformity. However, combined RFAE and other PFAE techniques for effective recovery of pectin have not been reported. Thus, to explore the potential of combined US and RF treatment as a new method for pectin extraction, the focus of this study was on applying the response surface method (RSM) for optimizing extraction parameters involved in sequential ultrasound-radio frequency-assisted extraction (URAE) of PPP to attain the maximum yield. Subsequently, based upon optimized URAE parameters, the yield, chemical, structure, and functional characteristics of pectin obtained from URAE, sequential combination of RFAE and UAE (i.e., radio frequency-ultrasound-assisted extraction (RUAE)), UAE, and RFAE were also compared.

## Materials and Methods

### Materials

Fresh golden honey pomelo was obtained from a local supermarket. After shaving the flavedo layer of peel, the albedo layer was peeled manually and soaked in boiling water for 3 min for blanching. Blanched PP was dried at 45 °C for 24 h. Then, dried PP was pulverized and passed through 80 mesh sieves. The resulting flour was kept in desiccators for further studies. Commercial citrus pectin (CCP) was bought from Yantai Andre Pectin Co. Ltd., China. Reagents used in this study were purchased from Sinopharm Chemical Reagent Co., Ltd. (Shanghai, China) or Sigma-Aldrich (St. Louis, MO, USA).

### Pectin Extraction

#### Sample Preparation

Five grams of PP flour was dissolved in a Pyrex glass tube (inner,  $\varnothing$  55 mm  $\times$  h 100 mm) with 150-mL water-citric acid solution (pH 1.5) to form a pomelo peel-acid solution mixture (PPASM). The above liquid/solid ratio and pH were chosen based on the previous studies on citrus fruit pectin extraction (Wandee et al., 2019).

### URAE Procedure and Optimization

URAE includes a sequential combination of US and RF treatment (Fig. 1). Among them, US was carried out using an ultrasonic cell crusher (Xinyi-650N, Ningbo Xinyi Ultrasonic Equipment Co., Ltd. Ningbo, China) equipped with a flat type tip probe (6 mm diameter) operated at 20 kHz and maximum power of 650 W, which was connected to a digital control system for adjusting sonication time and power. The probe was immersed 1.0 cm with respect to the PPASM surface loaded in a glass tube. Sonication was conducted on different power inputs and time durations under pulsed mode (2 s on/2 s off) without temperature control. Immediately after US treatment, the glass tube was covered with a wooden lid and then placed on the center of the bottom electrode of an RF heater (Labotron RF2400, Sairem, Neyron, France, 27.12 MHz, 2.4 kW). Different RF heating rates of the sample can be obtained by changing the parallel electrode gap from 5.0 to 25.0 cm by the movable top electrode (39.0 cm × 59.0 cm). During RFAE, the electrode gap of 12.5 cm was used to obtain a fast heating rate of about 10 °C/min, and the real-time temperature at the geometry center of the PPASM (cold spot determined by pre-experiment) was recorded using a fiber-optic temperature sensor (HQ-FTS-D1F00, Heqi Technologies Inc., Xian, China). After reaching the set temperatures, the RF heater was switched on and off to maintain the temperature for a designated time, and then, PPASM was removed and cooled to room temperature using ambient natural air.

Four factors and three levels of the Box-Behnken design (BBD) experiment were employed to investigate and optimize the effect of process variables including sonication power (65–195 W) and time (10–30 min), RF heating temperature (70–90 °C), and holding time (5–25 min) on the maximum PY (Cilingir et al., 2023; Zheng et al., 2021). The whole design consisted of 29 experimental points, including 24 factorial points and 5 center points (used to evaluate experimental errors), which are listed in Table 1. The experimental design and data analysis were performed using Design Expert Software 8.0 (Stat-Ease Inc., Minneapolis, USA). The mean values of PY were fitted to a quadratic polynomial model as below:

$$PY = \beta_0 + \sum_{j=1}^k \beta_j X_j + \sum_{j=1}^k \beta_{jj} X_j^2 + \sum_i \sum_{j=2}^k \beta_{ij} X_i X_j \quad (1)$$

where PY is the predicted response;  $X_i$  and  $X_j$  are the independent variables;  $\beta_0$ ,  $\beta_j$ ,  $\beta_{jj}$ , and  $\beta_{ij}$  are the coefficients of the model; and  $k$  is the number of independent variables.

### UAE, RFAE, and RUAE Procedure

Extraction studies were also conducted using UAE, RFAE, and RUAE for comparison with URAE (Fig. 1). In the sole UAE and RFAE, the PPASM was treated only with US and RF treatment, respectively, as described in the “URAE Procedure and Optimization” section. In RUAE, the PPASM was heated by RF energy before US treatment. All the above three extractions were conducted according to the optimal

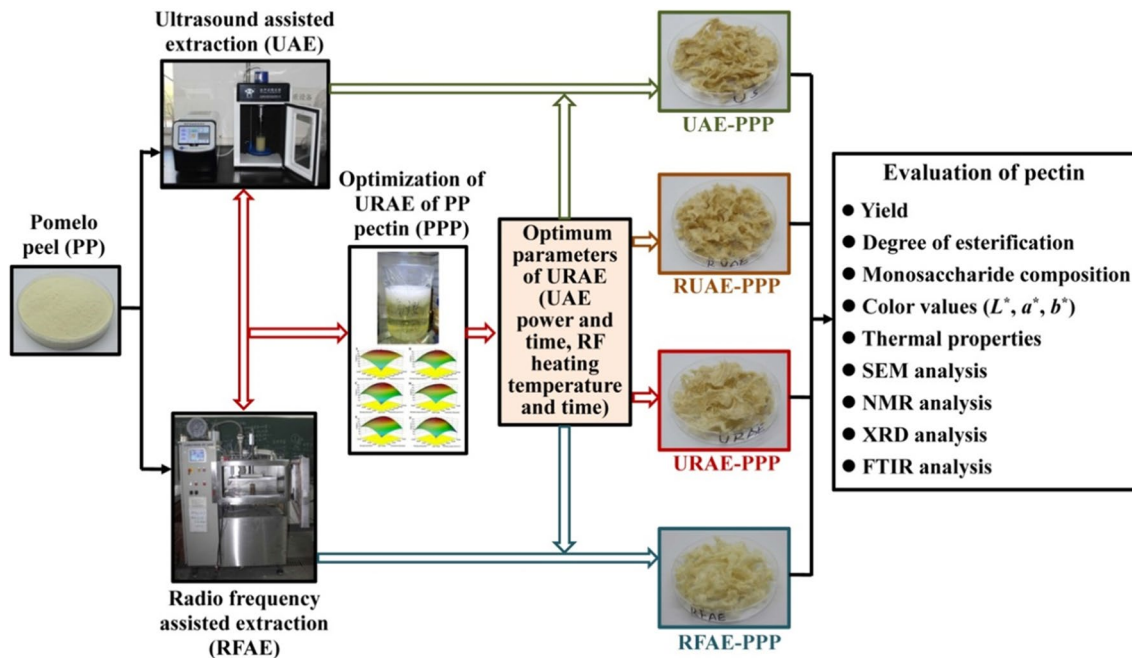


Fig. 1 Flow diagram of experimental designs

**Table 1** Independent factors and their levels for RSM and BBD experimental designs with experimental data and predicted values

Factors	Unit	Actual levels			PY <sub>exp</sub>	PY <sub>pred</sub>
		-1	0	1		
Sonication power (SP, X <sub>1</sub> )	W	65	130	195		
Sonication time (St, X <sub>2</sub> )	min	10	20	30		
RF heating temperature (RFT, X <sub>3</sub> )	°C	70	80	90		
RF heating time (RFt, X <sub>4</sub> )	min	5	15	25		
Run numbers	Variable levels				PY <sub>exp</sub>	PY <sub>pred</sub>
	SP-X <sub>1</sub>	St-X <sub>2</sub>	RFT-X <sub>3</sub>	RFt-X <sub>4</sub>		
1	65	20	90	15	20.05 ± 0.79	19.50
2	195	10	80	15	23.26 ± 1.76	23.95
3	195	20	80	25	26.62 ± 0.57	26.94
4	65	10	80	15	17.41 ± 0.99	17.54
5	130	10	80	5	18.42 ± 0.58	17.90
6	65	20	70	15	18.47 ± 0.21	18.78
7	130	20	80	15	26.97 ± 0.85	26.35
8	65	30	80	15	24.67 ± 1.24	23.58
9	130	10	80	25	22.90 ± 0.97	21.50
10	130	20	80	15	26.17 ± 0.15	26.35
11	195	20	80	5	20.02 ± 1.83	19.64
12	130	20	90	25	26.55 ± 0.55	26.33
13	130	20	70	25	19.41 ± 2.41	19.40
14	130	30	90	15	25.08 ± 0.48	25.64
15	130	30	80	25	26.72 ± 1.20	27.07
16	130	30	80	5	18.98 ± 0.03	20.20
17	130	20	70	5	18.02 ± 1.30	17.84
18	195	20	70	15	20.19 ± 0.53	20.56
19	130	20	80	15	25.45 ± 0.23	26.35
20	130	10	90	15	20.19 ± 0.81	21.27
21	130	10	70	15	18.43 ± 1.24	18.45
22	130	20	80	15	26.52 ± 0.55	26.35
23	65	20	80	25	19.62 ± 0.58	20.57
24	65	20	80	5	17.15 ± 0.33	17.40
25	195	20	90	15	26.83 ± 0.92	26.34
26	130	30	70	15	22.47 ± 1.19	21.96
27	130	20	80	15	26.65 ± 1.18	26.35
28	130	20	90	5	17.81 ± 1.48	17.42
29	195	30	80	15	26.31 ± 0.47	25.79

PY<sub>exp</sub> and PY<sub>pred</sub> are experimental and predicted pectin yields, respectively

URAE parameters reported in the “URAE process optimization by BBD” section, and the cooling operation was conducted after the four extraction methods.

### Purification of Pectin

Crude pectin filtrate was mixed with 95% ethanol at a volume ratio of 1:2 under ambient conditions for 12 h to full

precipitation of pectin. Precipitated pectin was separated by centrifuging, washed three to four times with ethanol, and then dried to constant weight. Dried pectin was weighed and the yield of pectin (%) was calculated on the dry mass of the PP sample. PPP was ground and sifted through 80 mesh sieves to obtain a fine powder (Kumari et al., 2023).

## Physicochemical Properties Analysis

### Degree of Esterification (DE)

The DE of extracted PPP was determined by a titration method according to Thu Dao et al. (2021). Briefly, 30-mg PPP flour was dissolved in 30 mL hot (40 °C) carbon dioxide-free water. The resulting solution was titrated against 0.1 mol/L sodium hydroxide ( $V_1$ , mL) using phenolphthalein as the indicator of the end point. Then, 5 mL sodium hydroxide (0.1 mol/L) was added and held for 20 min to further hydrolyze the side ester groups. Subsequently, 5 mL HCl (0.5 mol/L) was added and titrated with NaOH (0.1 mol/L,  $V_2$ , mL) to faint pink that persisted after shaking. The DE was calculated using Eq. (2):

$$DE(\%) = \frac{V_2}{V_1 + V_2} \times 100\% \quad (2)$$

### Monosaccharide Composition

Monosaccharide composition was determined using high-performance liquid chromatography (HPLC) method as described in Lin et al. (2021) with some modifications. A 5-mg pectin sample was hydrolyzed using 2 mL trifluoroacetic acid (2 mol/L) at 110 °C for 6 h. The dissolved samples were dried by  $N_2$  blowing and then added into 1 mL 0.3 mol/L NaOH and 0.4 mL 1-phenyl-3-methyl-5-pyrazolone-methanol (0.5 mol/L). After reacting at 70 °C for 2 h, the mixture was cooled and neutralized with HCl (0.3 mol/L). The final solution was extracted by chloroform two times, and the aqueous layer was filtrated through a 0.45- $\mu$ m membrane before performing the monosaccharide analysis with a ThermoFisher U3000 HPLC system coupled with a UV detector and equipped with a C18 column (250 $\times$ 4.6 mm, 5- $\mu$ m particle size, Japan). The mobile phase consisted of 0.1 mol/L sodium phosphate buffer (phase A, pH 6.6) and acetonitrile (phase B). The flow rate, injection volume, column temperature, and UV detection wavelength were set to 1 mL/min, 5  $\mu$ L, 30 °C, and 245 nm, respectively. Different concentrations of monosaccharide solutions were used as standards.

### Thermal Analysis

Differential scanning calorimeter (DSC Q2000, TA Instruments, New Castle, DE, USA) was used for the analysis of the thermal properties of PPPs according to Tunç and Odabaş (2021). Briefly, 0.1-mg PPP flour was added to an aluminum pan and an empty pan was used as a reference. Then, the pan was hermetically sealed and heated from 30 to 300 °C at a rate of 10 °C/min.

### Color Values

Colorimeter (CS-210, CHNSpec Technology Co., Ltd., Hangzhou, China) was used to determine the PPP color, and the results were expressed as CIE LAB system ( $L^*$ ,  $a^*$ , and  $b^*$ ) values.

### Functional Properties

Functional properties including total phenolic content (TPC), antioxidant capacity (AC), water (WHC)/oil (OHC) holding capacities, emulsifying capacity (EC), and stability (ES) were determined, and the CCP was used for comparative study. Among them, TPC and AC were determined as described by Zheng et al. (2021) using Folin-Ciocalteu and DPPH free radical method, respectively, and the results were expressed as mg GAE/g pectin and Trolox equivalent antioxidant capacity values (TEAC,  $\mu$ mol Trolox/g pectin). WHC and OHC were determined according to the method of Yang et al. (2024), and the results were expressed as the g water/oil/g pectin. EC and ES were determined according to the method of Wang et al. (2021).

### Structural Characterization

#### Fourier-Transform Infrared Spectroscopy (FTIR) Analysis

Infrared spectrometer (Vetex70, BRUKER Inc., Munich, Germany) was used to analyze the FTIR spectra of PPP in the range of 4000 to 400  $cm^{-1}$  with 16 scans at a resolution of 4  $cm^{-1}$ .

#### X-Ray Diffraction (XRD) Analysis

Diffractionmeter (D8 Advance A25, BRUKER Inc., Germany) was used to analyze the amorphous and crystalline nature of PPP according to Li et al. (2020). Briefly, 5-mg PPP flour was scanned at room temperature with a diffraction angle ( $2\theta$ ) in the range of 10–50° with a step size of 0.05°/s.

#### Nuclear Magnetic Resonance Spectroscopy (NMR) Analysis

NMR spectrometer (AVANCE III-500 MHz, BRUKER Inc., Karlsruhe, Germany) was used to analyze the  $^1H$  NMR spectrum of PPP according to Rahmani et al. (2020). Twenty milligrams of PPP flour was dissolved in  $D_2O$ , and the scanning was carried out at 25 °C, 32 scans with a relaxation delay of 1 s and acquisition time of 4 s.

#### Surface Morphology Analysis

The surface morphology of PPP was examined by a scanning electron microscope (SEM, S-3400N, Hitachi, Ltd, Tokyo, Japan) according to Jamshidi et al. (2024). PPP flour was fixed to the sample table with double-sided adhesive tape and coated



with gold. SEM analysis was carried out using an accelerating voltage of 5 kV with a magnification of 500 and 1000 $\times$ .

### Statistical Analysis

All determinations were performed in triplicate unless otherwise stated, and the results were expressed as the mean  $\pm$  standard deviations. Statistical differences were analyzed using SPSS (V18.0, SPSS Inc., Chicago, IL, USA) following the analysis of variance and Tukey's honestly significant difference (HSD) test ( $p < 0.05$ ).

$$\begin{aligned} \text{PY (\%)} = & 26.35 + 2.15X_1 + 1.97X_2 + 1.63X_3 + 2.62X_4 - 1.05X_1X_2 + 1.26X_1X_3 \\ & + 1.03X_1X_4 + 1.84X_3X_4 - 2.08X_1^2 - 1.55X_2^2 - 2.97X_3^2 - 3.13X_4^2 \end{aligned} \quad (3)$$

As shown in Table 2, the high  $R^2$  (0.970), adjusted  $R^2$  (0.940), and predicted  $R^2$  (0.843) indicated the high ability of the model to explain the relationship between independent variables and response in a precise manner, and there was no need for higher order models. Moreover, the results showed that the effects of the variables including all linear terms ( $p < 0.001$ ) and quadratic terms ( $p < 0.05$ ) and four mutual interactions (SP-St, SP-RFT, SP-RFt, and RFT-RFt,  $p < 0.05$ ) were significant on the PY. As shown in Fig. 2, 3D response surface plots (factor not shown was fixed at level 0) were used to illustrate the relationship between yield and experimental levels of each factor and the mutual interactions between each two tested factors.

As shown in Fig. 2A–C, the PY increased when sonication power moderately raised with sonication time and RF heating temperature/time and reached the highest value around 180 W, while beyond this value, the PY decreased with increasing of other variables especially for RF heating with higher temperature and longer time. Similarly, the sonication time showed the same trends, and the highest PY was obtained around 25 min as shown in Fig. 2A, D, and E. Initially, since US treatments improved the swelling of cellular matrix, expanded the matrix porosity, and loosened the structure, PY increased gradually with increasing the extension of sonication time or sonication power, while above a certain processing intensity, the PY decreased slightly with increasing of sonication treatment, which may be due to the fact that the overexposure to US treatment leads to the degradation of pectin macromolecules, and also the swelling effect of US leads to the formation of high-viscosity regions that hinders further dissolution of the pectin (Wang et al., 2017). Furthermore, the quadratic effects of RF heating temperature on PY could be found in Fig. 2B, D, and F, showing that increasing temperature led to the increase of yield rapidly at first and then slowly or decreased significantly. The

## Results and Discussions

### URAE Process Optimization by BBD

Multiple regression analysis was carried out on the experimental data of URAE (Table 2), and a second-order polynomial model with significant fit ( $p < 0.001$ ) and insignificant lack of fit ( $p > 0.05$ ) were successfully developed. The developed model in terms of coded variables (as listed in Table 1) is given below:

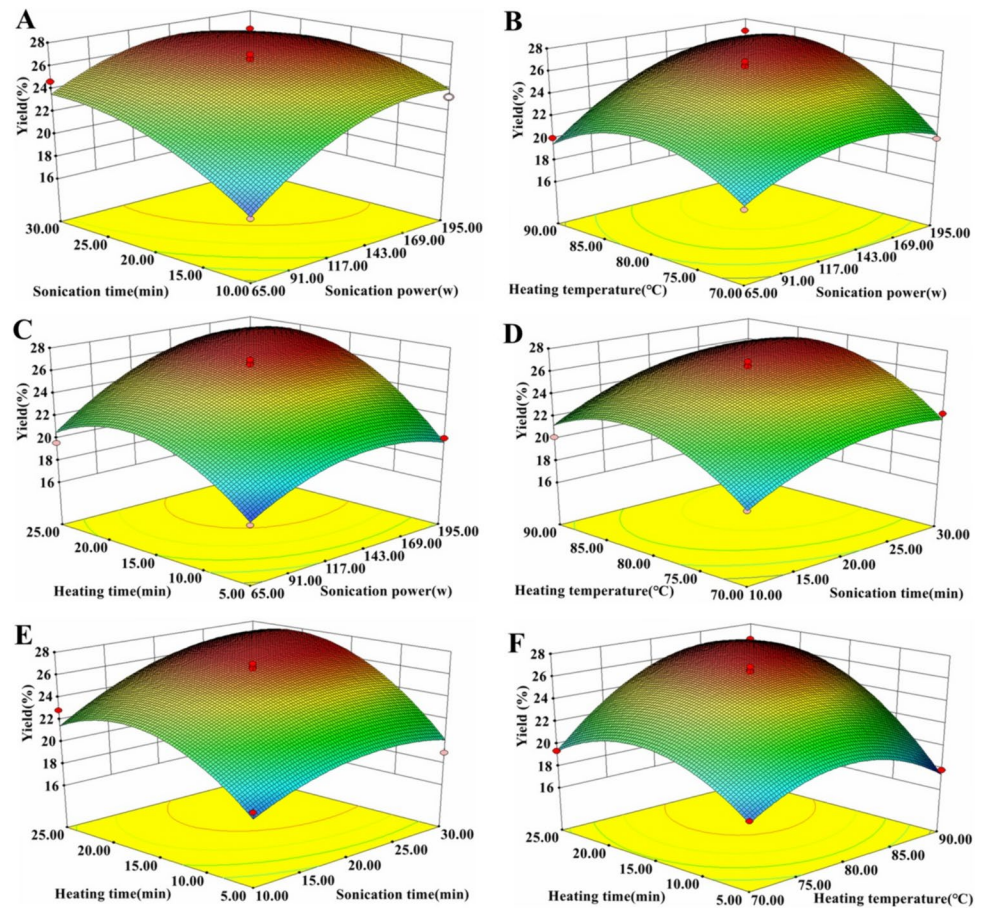
PY reached a peak at the RF heating temperature of around 85 °C. Higher temperature can promote extraction, while an elevated temperature also critically reduced the pectin yield due to thermal degradation (Zheng et al., 2021). The optimal RF heating time to obtain the highest PY was around 20 min. Enhanced PY at longer RF heating time may be attributed to more dissolution and release of pectin from the plant matrix into the solution as a result of greater extraction times (Gharibzahedi et al., 2019a).

**Table 2** Analysis of variance (ANOVA) for the proposed model of PY

Source	Sum of squares	DF	Mean square	F-value	p-value
Model	359.18	14	25.66	32.36	<0.0001
SP*	55.73	1	55.73	70.28	<0.0001
St	46.49	1	46.49	58.63	<0.0001
RFT	31.75	1	31.75	40.04	<0.0001
RFt	82.27	1	82.27	103.75	<0.0001
SP $\times$ St	4.43	1	4.43	5.59	0.0331
SP $\times$ RFT	6.40	1	6.40	8.07	0.0131
SP $\times$ RFt	4.26	1	4.26	5.38	0.0360
St $\times$ RFT	0.18	1	0.18	0.23	0.6405
St $\times$ RFt	2.66	1	2.66	3.35	0.0885
RFT $\times$ RFt	13.51	1	13.51	17.03	0.0010
SP $\times$ SP	28.16	1	28.16	35.51	<0.0001
St $\times$ St	15.65	1	15.65	19.74	0.0006
RFT $\times$ RFT	57.26	1	57.26	72.21	<0.0001
RFt $\times$ RFt	63.59	1	63.59	80.19	<0.0001
Residual	11.10	14	0.79		
Lack of fit	9.76	10	0.98	2.90	0.1583
Pure error	1.35	4	0.34		
Cor total	370.28	28			
$R^2$	0.97	Adj $R^2$	0.94	Pred $R^2$	0.8426

\*SP sonication power, St sonication time, RFT RF heating temperature, RFt RF heating time

**Fig. 2** Response surface plots showing the effects of independent variables on the PY (A sonication time  $\times$  sonication power; B heating temperature  $\times$  sonication power; C heating time  $\times$  sonication power; D heating temperature  $\times$  sonication time; E heating time  $\times$  sonication time; F heating time  $\times$  heating temperature)



From the developed second-order polynomial model Eq. (3), the optimum conditions on maximum predicted PY (29.13%) are sonication power of 183.32 W with a holding time of 23.55 min and RF heating at 86.82 °C with a holding time of 22.53 min. For validation, three verification experiments were carried under the predicted optimal conditions using its modified form (sonication treatment, 183 W/24 min; RF treatment, 87 °C/23 min), and the result ( $28.36 \pm 0.85\%$ ) was closely related to the predicted value, which means that the developed model was adequate for prediction of the yield during URAE. Therefore, the above modified form was used for RUAE, UAE, and RFAE.

### Comparison of PY Using Different Methods

Although a lot of studies reported that US is an efficient intensification technique and can be used alone or as a pretreatment for subsequent processing, few studies have been focused on the effect of sequencing orders on the performance of UAE combined with other PFAE techniques. As shown in Table 3, URAE obtained the highest yield as compared to other methods. It is generally considered that the cavitation phenomenon induced by US can disrupt the cell walls and facilitate the extract release, and the following thermal treatment (e.g., RF heating raises the system

temperature rapidly) accelerates the mass transfer of extract (Khedmat et al., 2020), while under the reverse order, the yield of RUAE was significantly lower than that of URAE and was slightly higher than that of sole RFAE, indicating that RF heating effect may be dominant in the RUAE process. This may be due to the overlapping of US cavitation and RF thermal effect; thus, the enhancement role of US was not as distinct as that in the URAE process. Furthermore, according to Wang et al. (2017), pectin is sticky, and the swelling volume increases with the US treatment, which leads to relatively high-viscosity regions that hinder further dissolution of the pectin and result in an incomplete extraction. Thus, the significantly lower PY of RUAE may be also due to the formation of a high-viscosity stagnant layer in the second extraction stage, and this also explains why sole UAE obtained a much lower yield as compared to other methods. Compared with similar studies, Liew et al. (2016) reported that the yield of UMAE of PPP was significantly higher than that of MUAE using the same operating parameters. However, Tien et al. (2022) also reported that MUAE provided the highest yield as compared to UMAE, sole MWAE, and UAE during pectin extraction from dragon fruit peel, which may be due to the fact that the operation parameters used in exploring the extraction effects in different sequences are different from ours. In addition, compared

with other studies related to the citrus peel pectin extraction, Liew et al. (2016) reported that the PY from PP was 14.25% for the UAE alone, while 36.33% was obtained under the optimized UMAE condition. In another study, the PY from lemon peel can be reached 28.7% for the UAE alone (Panwar et al., 2023). Further, Wandee et al. (2019) also reported that the PY from PP was 20.5% for the MWAE alone. Difference results may be mainly due to the differences in the raw materials and experimental conditions. Based on the above results, sequential using US and RF treatment in combination with citric acid extraction is a strategic procedure to have a considerable yield of pectin from plant sources.

### Comparison of Different Extraction Methods on Physicochemical Properties

#### DE

Pectin quality can be evaluated based on the DE because this chemical parameter is related to its gelling ability. As shown in Table 3, all the extracted PPP belonged to high methoxyl pectin (HMP) because DE were higher

than 50%, indicating that PPP can be used as a gelling agent or for other food applications. Among them, the DE values of combined extractions were significantly lower than those of sole extraction, and the lowest and highest values were observed in URAE and UAE, respectively. It is generally considered that the harsher extraction conditions may promote the de-esterification of polygalacturonic chains, resulting in lower DE (Su et al., 2019). Thus, the reduction of DE in combined extractions may be due to the prolonged exposure at high temperatures, especially in RUAE (as US treatment was conducted at high temperatures due to RF heating).

#### Monosaccharide Component

Regarding the monosaccharide composition (Table 3), no changes can be observed in the types of monosaccharides of pectin extracted by different methods except for some differences in their ratios. All pectins mainly consist of GalA, which is the major backbone of the pectin structure with  $\alpha$ -1,4 linkages, and there were various types of neutral

**Table 3** Yield and characteristics of PPP extracted by different methods

Pectin characteristics	Extraction method <sup>1</sup>			
	URAE	RUAE	UAE	RFAE
PY (%)	28.36 ± 0.85 <sup>a2</sup>	22.32 ± 0.69 <sup>b</sup>	13.68 ± 0.62 <sup>d</sup>	20.25 ± 0.74 <sup>c</sup>
DE (%)	56.2 ± 1.7 <sup>c</sup>	58.1 ± 2.3 <sup>c</sup>	70.6 ± 2.2 <sup>a</sup>	64.1 ± 1.7 <sup>b</sup>
Monosaccharide content (% w/w) <sup>3</sup>				
Galacturonic acid (GalA)	52.2 ± 2.8 <sup>a</sup>	54.1 ± 1.13 <sup>c</sup>	45.9 ± 2.9 <sup>e</sup>	45.9 ± 1.13 <sup>b</sup>
Mannose (Man)	1.9 ± 2.3 <sup>a</sup>	2.3 ± 1.8 <sup>c</sup>	2.7 ± 2.4 <sup>e</sup>	2.3 ± 1.8 <sup>b</sup>
Rhamnose (Rha)	8.2 ± 2.4 <sup>a</sup>	4.9 ± 1.9 <sup>c</sup>	8.7 ± 2.5 <sup>e</sup>	6.8 ± 1.9 <sup>b</sup>
Arabinose (Ara)	15.5 ± 2.5 <sup>a</sup>	13.6 ± 1.10 <sup>c</sup>	16.9 ± 2.6 <sup>e</sup>	13.4 ± 1.1 <sup>b</sup>
Galactose (Gal)	10.5 ± 2.6 <sup>a</sup>	13.3 ± 1.11 <sup>c</sup>	9.1 ± 2.7 <sup>e</sup>	7.5 ± 1.1 <sup>b</sup>
Glucose (Glc)	11.7 ± 2.7 <sup>a</sup>	11.8 ± 1.12 <sup>c</sup>	16.8 ± 2.8 <sup>e</sup>	24.0 ± 1.2 <sup>b</sup>
Color values				
<i>L</i> <sup>*</sup>	62.6 ± 0.8 <sup>b</sup>	59.1 ± 0.5 <sup>c</sup>	56.3 ± 0.3 <sup>d</sup>	68.5 ± 0.3 <sup>a</sup>
<i>a</i> <sup>*</sup>	11.3 ± 0.2 <sup>b</sup>	15.0 ± 0.2 <sup>a</sup>	14.9 ± 0.5 <sup>a</sup>	8.6 ± 0.4 <sup>c</sup>
<i>b</i> <sup>*</sup>	20.1 ± 0.5 <sup>c</sup>	25.1 ± 0.3 <sup>a</sup>	23.7 ± 0.2 <sup>b</sup>	18.3 ± 0.2 <sup>d</sup>
Thermal parameters <sup>4</sup>				
<i>T</i> <sub>m</sub> (°C)	140.1 ± 3.3 <sup>b</sup>	150.8 ± 2.2 <sup>a</sup>	133.2 ± 1.9 <sup>c</sup>	148.8 ± 3.2 <sup>a</sup>
$\Delta H$ <sub>m</sub> (J/g)	49.8 ± 2.5 <sup>c</sup>	72.7 ± 3.1 <sup>a</sup>	44.1 ± 1.6 <sup>d</sup>	68.9 ± 2.7 <sup>b</sup>
<i>T</i> <sub>d</sub> (°C)	249.2 ± 4.9 <sup>a</sup>	245.9 ± 3.7 <sup>a</sup>	247.9 ± 6.2 <sup>a</sup>	247.1 ± 4.3 <sup>a</sup>
$\Delta H$ <sub>d</sub> (J/g)	142.8 ± 2.2 <sup>a</sup>	135.2 ± 4.1 <sup>b</sup>	141.8 ± 3.4 <sup>a</sup>	140.8 ± 5.8 <sup>a</sup>

<sup>1</sup>Extracting conditions in an acidic medium (pH 1.5) with liquid/solid ratio of 30: URAE (183 W/24 min + 87 °C/23 min), RUAE (87 °C/23 min + 183 W/24 min), UAE (183 W/24 min), RFAE (87 °C/23 min)

<sup>2</sup>Means within a row among the different extractions followed by same lower-case letters are not significantly different at the 5% probability level

<sup>3</sup>% expressed over total identified monosaccharides

<sup>4</sup>Total contents of neutral sugars were calculated as sum of Man, Rha, Ara, Gal, and Glc

<sup>5</sup>*T*<sub>m</sub>, temperature of melting;  $\Delta H$ <sub>m</sub>, melting enthalpy; *T*<sub>d</sub>, temperature of degradation;  $\Delta H$ <sub>d</sub>, degradation enthalpy



sugars with different ratios. Among them, URAE and RUAE had higher and statistically similar GalA contents, which might be because combined extraction was able to separate pectin from the plant matrix more completely than sole extraction. A similar phenomenon was also observed in pectin extraction from tomato peel and fig skin that an increase of yield by combined MWAE and UAE was also accompanied by an increase of GalA (Gharibzadeh et al., 2019a; Sengar et al., 2020). Major components of neutral sugars were Ara, Gla, and Glc for all samples, while the Rha and Man were the least. Another study confirmed that acid-extracted (pH ~ 1.5) PPP mainly consisted of Ara followed by Gal and Glc (Wandee et al., 2019). Compared with sole UAE or RFAE, combined extractions (URAE and RUAE) resulted in lower contents of total neutral sugars, indicating the occurrence of degradation of some side chains of neutral sugars, which may be due to the harsh conditions during combined extraction (Yang et al., 2019).

## Color

Color is a key index that determines the application of pectin in food processing. As shown in Table 3, RFAE pectin showed the highest *L* (lightness) and lowest *a* (red-green) and *b* (yellow-blue) values among four samples, and this observation corresponds with the macrograph of the RFAE sample (i.e., appears whiter and brighter) as shown in Fig. 1, while for other three pectins, it all appears dark yellow, especially for UAE and RUAE. PP contains high levels of flavonoids and carotenoids, and both of them may be responsible for the color of PPP (Tocmo et al., 2020). During pectin

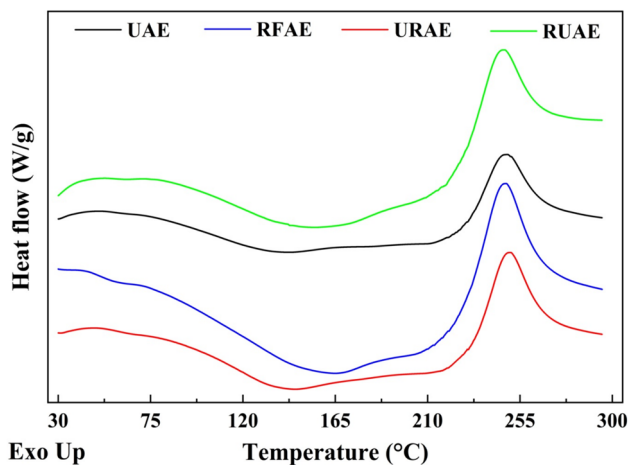


**Fig. 3** DSC images of PPP extracted by different methods (UAE, RFAE, URAE, and RUAE indicated the ultrasound-assisted extraction, radio frequency-assisted extraction, ultrasound-radio frequency-assisted extraction, and radio frequency-ultrasound-assisted extraction, respectively)

extraction, the disintegration of the cell matrix makes water-soluble pigments dissolved in the solvent, while the part of water/ethanol insoluble flavonoids and carotenoids may be trapped in pectin during alcohol precipitation. Considering that all the pectins were purified under the same conditions, the lower *L* value and dark yellow color were observed in all three US-treated samples, indicating that sole UAE or a combination of UAE and RFAE was more efficient for the release of pigments from deeper parts of plant matrix.

## Thermal Properties

The thermal behavior of PPP extracted by different methods was analyzed by DSC between 30 and 300 °C. DSC curves and their related parameters are shown in Fig. 3 and Table 3, respectively. All curves were similar in shape and showed two regions around 140 °C and 240 °C, and similar regions were also observed in other citrus fruits pectin recovered by UAE and subcritical water (Wang et al., 2016). The first region ranging from 130 to 150 °C was an endothermic peak ( $T_m$ , melting temperature), which can be generally considered a slight weight loss due to the evaporation of absorbed water in pectins as the temperature increased. Among them, RUAE and RFAE showed larger  $T_m$  and heat flow ( $\Delta H_m$ , melting enthalpy) as compared to the other two samples, indicating that these two samples contain more hydrophilic groups and have stronger water holding capacity. The second region ranging from 245 to 250 °C was an exothermic peak ( $T_d$ , degradation temperature);  $T_d$  generally corresponded to the degradation of pectin in the thermal processing. As shown in Table 3, there were no significant differences observed in  $T_d$  among all four samples, except that degradation enthalpy ( $\Delta H_d$ ) of RUAE was slightly lower, indicating that the thermal stability of pectin recovered by the four methods was the same. Although the effect of combined acoustic and electromagnetic field extraction on the thermal behavior of pectin has not been reported, no significant differences in the thermal stability of pectins recovered by sole UAE and MWAE have been reported by Dranca et al. (2020). Overall, PPPs from all four extraction methods were concluded to be more suitable for food product applications involving process temperatures of lower than 200 °C.

## Comparison of Different Extraction Methods on Functional Properties

TPC is an important parameter that could affect the AC of pectin. As shown in Table 4, the mean TPC values of all four PPPs (6.6–10.3 mg GAE/g) were significantly higher than those of CCP (1.2 mg GAE/g), and among them, RFAE was the highest while RUAE was the lowest. Similarly, for AC, all four PPPs (9.8–16.6  $\mu\text{mol Trolox/g}$ )

**Table 4** Functional properties of PPP extracted by different methods

Functional properties	Extraction method <sup>1</sup>				
	CCP	URAE	RUAE	UAE	RFAE
TPC (mg GAE/g)	1.2±0.3 <sup>a2</sup>	7.5±0.6 <sup>b</sup>	6.6±0.4 <sup>b</sup>	8.7±0.3 <sup>c</sup>	10.3±0.5 <sup>d</sup>
DPPH (μmol Trolox/g)	2.6±0.2 <sup>a</sup>	11.2±0.4 <sup>c</sup>	9.8±0.5 <sup>b</sup>	14.9±0.6 <sup>d</sup>	16.6±0.4 <sup>c</sup>
WHC (g/g)	2.8±0.3 <sup>a</sup>	4.0±0.2 <sup>b</sup>	3.6±0.3 <sup>b</sup>	3.5±0.4 <sup>b</sup>	3.7±0.3 <sup>b</sup>
OHC (g/g)	2.2±0.2 <sup>a</sup>	3.0±0.2 <sup>b</sup>	2.7±0.1 <sup>b</sup>	2.6±0.4 <sup>ab</sup>	2.7±0.2 <sup>b</sup>
EC (%) <sup>3</sup>	18.5±0.5 <sup>a</sup>	21.6±0.4 <sup>b</sup>	22.2±0.3 <sup>b</sup>	23.1±0.2 <sup>c</sup>	24.7±0.5 <sup>d</sup>
ES (%) <sup>3</sup>	20.2±0.7 <sup>a</sup>	24.8±0.2 <sup>c</sup>	23.1±0.5 <sup>b</sup>	24.2±0.4 <sup>c</sup>	25.5±0.3 <sup>d</sup>

<sup>1</sup>Extracting conditions in an acidic medium (pH 1.5) with liquid/solid ratio of 30: URAE (183 W/24 min+87 °C/23 min), RUEA (87 °C/23 min+183 W/24 min), UAE (183 W/24 min), RFAE (87 °C/23 min)

<sup>2</sup>Means within a row among the different extractions followed by same lower-case letters are not significantly different at the 5% probability level

<sup>3</sup>The emulsion solutions were prepared by adding 4 mL of olive oil to 4 mL of pectin solution (0.5%, w/v)

were also significantly higher than CCP (2.6 μmol Trolox/g) with RUEA as the lowest. This result may be attributed to most of the polyphenols in CCP having been removed during the refining process, while the samples obtained in our study were crude pectin with more polyphenols retained and shown stronger AC. It is worth noting that the TPC and AC of samples obtained from the extractions involved UAE were significantly lower than RFAE alone, which may be due to the better cavitation effect of US, resulting in the losses of most polyphenols into the extraction solution (Tao et al., 2022). On the whole, the values of TPC obtained in our study were lower than the similar studies for citrus pectin reported by Panwar et al. (2023). On the one hand, this may be due to the difference in material varieties, and on the other hand, the flavedo layer of PP was shaved before the experiment in our study, which contains most of the polyphenols in citrus peel as reported by Tocmo et al. (2020).

WHC/OHC represented the amount of water/oil absorbed by pectin and reflected the essential features of hydrocolloids (Cui et al., 2021). In this work (Table 4), the WHC and OHC of four PPP samples were between 3.5 to 4.0 and 2.6 to 3.0 g/g, respectively, but there was no significant difference ( $p > 0.05$ ) between each other. These values were slightly lower than the values of citrus peel pectin extracted using manosonication reported by Hu et al. (2021) but higher than the citrus limetta peel pectin extracted using UAE reported by Panwar et al. (2023). Compared with CCP, there was a significant increase ( $p < 0.05$ ) in WHC and OHC for all four PPPs. A similar phenomenon was also observed in mandarin peel pectin extracted using induced electric field heating reported by Yang et al. (2024). Thus, this result implies that PPPs extracted from UAE or RFAE or a combination of both methods with an adequate WHC/OHC value could be a good stabilizer and emulsifier in food systems with high moisture/fat content.

The emulsifying properties including the EC and ES of CCP and PPPs were examined in an oil/water emulsion system, and the results are listed in Table 4. The ECs

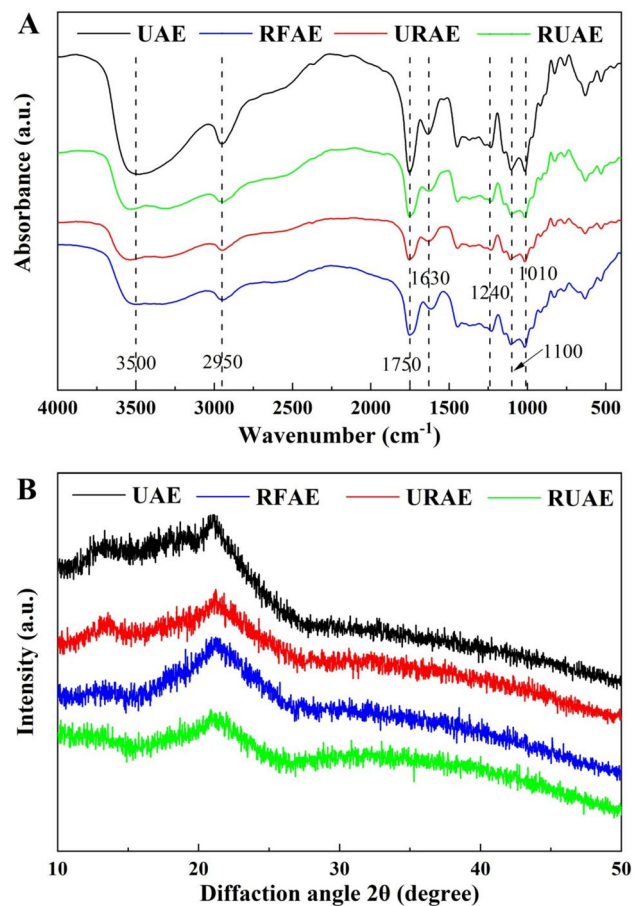


**Fig. 4** FTIR spectra (A) and XRD patterns (B) of PPP extracted by different methods (UAE, RFAE, URAE, and RUEA indicated the ultrasound-assisted extraction, radio frequency-assisted extraction, ultrasound-radio frequency-assisted extraction, and radio frequency-ultrasound-assisted extraction, respectively)

of PPPs ranged from 21.6 to 24.7%, which were higher than that of the CCP (18.5%). The highest EC (24.7%) was found in RFAE, while URAE was the lowest (21.6%). These results may be attributed to the diffusion rate of US-treated pectins at the O/W interface, which was higher than that of untreated ones, which stabilized the emulsion droplets and prevented the droplet accumulation in the emulsion. Similar results were also observed in US-treated citrus pectin reported by Wang et al. (2021). Meanwhile, Table 4 shows that the ES of PPPs obtained from different extraction methods ranged from 23.1 to 25.5%, which were higher than that of CCP (20.2%) and that RFAE had the highest ES. Based on the above-mentioned results, we can conclude that UAE or RFAE or a combination of both methods may enhance the emulsifying property of pectin-prepared O/W emulsions.

### Comparison of Different Extraction Methods on Structural Properties

FTIR is a fast and convenient method to analyze the chemical structure of polysaccharides. FTIR spectroscopy (Fig. 4A) shows a comparable spectrum for all four samples, the broad absorption peak around  $3500\text{ cm}^{-1}$  corresponding to the stretching vibration of  $-\text{OH}$  groups and the small absorption peak around  $2950\text{ cm}^{-1}$  due to  $-\text{CH}$  stretching of  $\text{CH}_2$  groups (Su et al., 2019). Another important region was between  $1500$  and  $1800\text{ cm}^{-1}$  related to the evaluation of the degree of methylation (Rodsamran & Sothornvit, 2019). Among them, the peak around  $1750$  and  $1630\text{ cm}^{-1}$  was common for pectin from all sources and

corresponded to the  $\text{C}=\text{O}$  stretching vibration of esterified carboxyl and free carboxyl groups, respectively. It is generally considered that increasing intensities and peak area of esterified carboxyl groups resulted in an increased DE. Thus, the significantly larger peak area at  $1750\text{ cm}^{-1}$  observed in UAE pectin indicated that it had a higher DE value as compared to other samples, which was consistent with the results determined by the chemical method as listed in Table 3. Furthermore, the band between  $1000$  and  $1400\text{ cm}^{-1}$  was collectively referred to as the fingerprint area for carbohydrates. All samples can observe three weaker absorption peaks at  $1010$ ,  $1100$ , and  $1240\text{ cm}^{-1}$ , which correspond to  $\text{C}-\text{O}-\text{C}$  glycoside ring bond stretching, and similar typical peaks were also observed in MWAE PPP (Wandee et al., 2019). Overall, the data obtained from spectroscopy indicated that the extracted samples were pectin and there were no significant differences in the main chemical structures among them.

To provide information about crystallization structure, the XRD patterns of PPP recovered using different methods were exhibited in Fig. 4B. It is generally considered that the crystallinity of pectin can be determined by the sharper and narrower diffraction peaks, while the absence of these peaks indicates the amorphous nature of the pectin. All four PPPs showed majorly non-crystalline (amorphous) and little crystallinity in nature with one major crystalline peak at  $20.7^\circ$ ,  $21.0^\circ$ ,  $21.4^\circ$ , and  $21.5^\circ$  in UAE, RFAE, URAE, and RUAE sample, respectively. A similar major crystalline peak was also observed in pectin recovered from sour orange and grapefruit peel using UAE (Hosseini et al., 2019; Wang et al., 2016).

**Fig. 5**  $^1\text{H}$  NMR spectra of PPP extracted by different methods (UAE, RFAE, URAE, and RUAE indicated the ultrasound-assisted extraction, radio frequency-assisted extraction, ultrasound-radio frequency-assisted extraction, and radio frequency-ultrasound-assisted extraction, respectively)

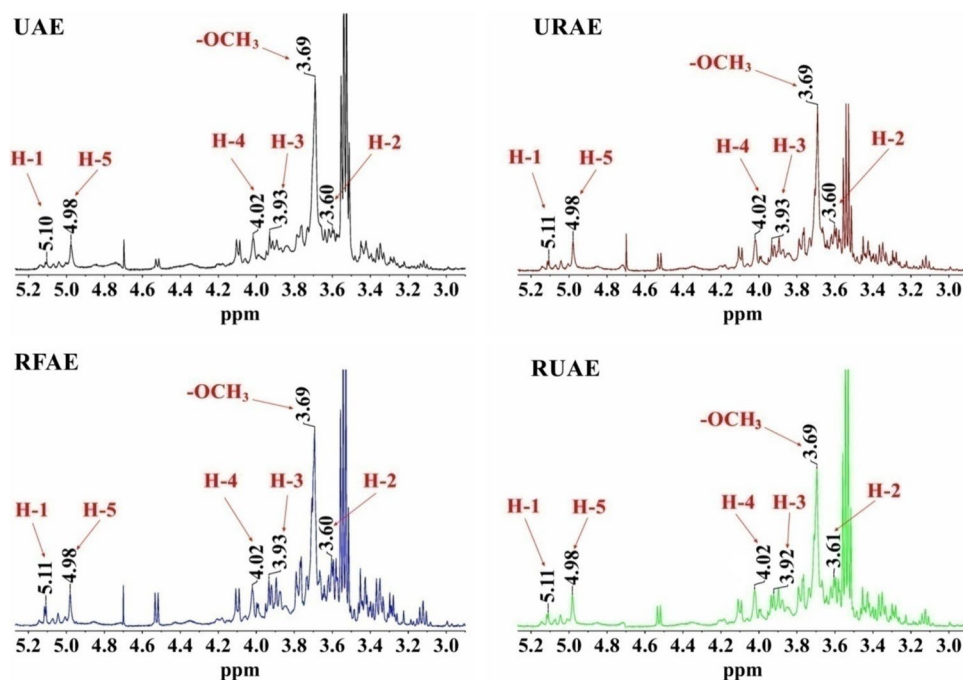
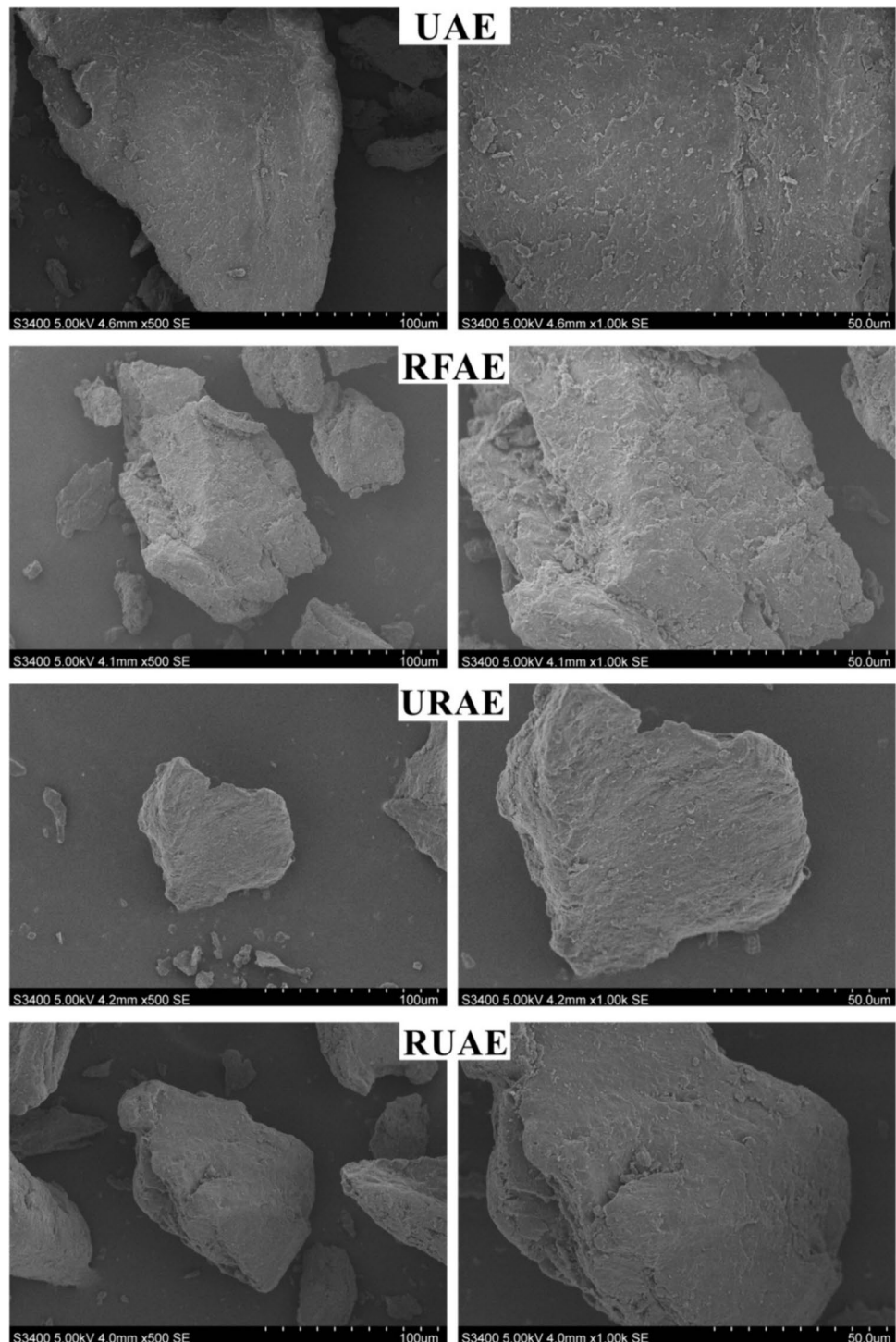




**Fig. 6** SEM images (left, 500 $\times$ ; right, 1000 $\times$ ) of PPP extracted by different methods (UAE, RFAE, URAE, and RUEA indicated the ultrasound-assisted extraction, radio frequency–assisted extraction, ultrasound–radio frequency–assisted extraction, and radio frequency–ultrasound–assisted extraction, respectively)



Furthermore, UAE showed other minor crystalline peaks at 20.7°, 21.1°, 26.3°, and 43.4°; RFAE at 19.1°, 20.5°, 23.4°, 25.7°, and 38.5°; URAE at 13.3°, 16.7°, 21.2°, and 33.9°; and RUEA at 18.7°, 32.1°, 43.1°, and 49.2°. Based on the XRD results, it could be concluded that the PPP recovered by a sequential combination of UAE and RFAE had similar non-crystalline structures, independent of the sequencing order.

To further analyze the structural characteristics of pectin extracted from different methods, the  $^1\text{H}$  NMR spectrum of PPP was also determined. As shown in Fig. 5, a sharp and strong chemical shift at 3.69 ppm observed in all four PPPs was probably caused by methoxy groups linking with the carboxyl groups of GalA (Yang et al., 2019). It is generally considered that the higher intensity of methoxy groups at around 3.7 ppm represents a high DE value



(Kazemi et al., 2019). Although all four pectins recovered from PP were classified as HMP, samples extracted by UAE and RFAE showed a relatively higher peak intensity at 3.69 ppm as compared to two other samples, which was in accordance with the DE values obtained from titrimetric and spectrometer methods. Other major signals in PPP assigned to the five protons in the D-galacturonic acid were H-1 5.10, H-2 3.60, H-3 3.93, H-4 4.02, and H-5 4.98 ppm, which was in agreement with previous study for citrus pectin reported by Hu et al. (2021). In all, the obtained results demonstrated the predominant presence of pectin structure in the obtained samples, and no significant differences were observed in the  $^1\text{H}$  NMR spectrum between PPP extracted using different methods except for the intensity of some peaks.

### Comparison of Different Extraction Methods on Surface Morphology

As shown in Fig. 6, pectin from sole UAE had a smoother and intact surface than other samples, while obvious cracking and wrinkled surface can be observed in samples from sole RFAE. Wang et al. (2015) reported that the smooth surface of pectin from UAE may be because the US treatment disrupted the crosslinks between pectin molecules and reorganized the pectin matrix. Regarding the RFAE, quick temperature increases and high internal pressure associated with RF volumetric heating not only led to the rupture of the cell wall and facilitated the pectin diffusion, but also had an obvious influence on its surface structure (Zheng et al., 2021). For the combined extractions, URAE showed a more compact, smoother, and flatter surface with less cracks than RUAE. Different morphological characteristics in pectin extracted under different sequential orders might be due to different dominant mechanisms. In the URAE process, US treatment promoted the swelling of the cell wall, and then, RF treatment accelerated the mass transfer, resulting in a relatively intact and smooth surface with a higher yield. While in the RUAE process, RF heating directly led to the disintegration of the cell wall, further incorporation of US treatment associated with swelling was less effective, thus forming relative cracking and wrinkled surface with lower yield. Based on the above analysis, the differences in the surface morphology of the PPPs explained the capability of the extraction conditions to destroy the cell wall, thereby leading to differences in the pectin yield.

### Conclusion

In this study, the BBD method was applied to optimize the URAE process for PPP extraction and evaluate the effects of four variables including sonication power and time, RF

heating temperature, and holding time on the yield. The yield was  $28.36 \pm 0.85\%$  under optimal conditions of citric acid pH of 1.5, sonication at 183 W for 24 min, and RF heating at  $87^\circ\text{C}$  for 23 min, which were significantly higher than those of RUAE, UAE, and RFAE using same extraction parameters. Among four extracted PPPs, URAE pectin showed lower DE (56.2%) but highest GalA content (54.1%) with the dark yellow color appearance. In addition, for the functional properties, the TPC and AC of RFAE showed the highest values, while URAE showed the best WHC and OHC with relatively lower WHC and OHC. On the whole, the functional properties of all four PPPs showed better functional properties than CCP. According to DSC analysis, no significant differences in thermal stability were observed in pectins recovered by different methods. Structure properties analysis using FTIR, XRD, and  $^1\text{H}$  NMR indicated that sequencing order did not alter the main chemical structures of pectin recovered by sequential combination of UAE and RFAE. Besides, SEM analysis showed that the surface morphology of URAE pectin was compact, smoother, and flatter surface with less cracks. Overall, the results suggested that sequential URAE was an effective way to raise the pectin extraction efficiency. However, further investigations are needed to explore the functional properties (e.g., interfacial, rheological, and gelling properties) and process costs, as a food ingredient before recommending the larger scale application of a sequential combination of UAE and RFAE.

**Author Contribution** Jin Wang: writing original draft, methodology, formal analysis. Hongyue Li, Sicheng Du: methodology, investigation, visualization, data curation. Shaojin Wang: writing review and editing. Bo Ling: funding acquisition, supervision.

**Funding** This study was supported by the Key Research and Development Project in Shaanxi Province of China (2023YBNY-150) and the National Natural Science Foundation of China (31901825).

**Data Availability** No datasets were generated or analysed during the current study.

### Declarations

**Competing Interests** The authors declare no competing interests.

### References

- Cilingir, S., Duran, G., Goekyildiz, B., Goksu, A., Sabanci, S., & Cevik, M. (2023). Optimization of pectin extraction from lemon peel powder by ohmic heating using full factorial design. *Food and Bioprocess Technology*, 17(3), 650–660. <https://doi.org/10.1007/s11947-023-03272-1>
- Cui, J., Zhao, C., Feng, L., Han, Y., Du, H., Xiao, H., & Zheng, J. (2021). Pectins from fruits: Relationships between extraction methods, structural characteristics, and functional properties. *Trends in Food Science and Technology*, 110, 39–54. <https://doi.org/10.1016/j.tifs.2021.01.077>
- Dranca, F., Vargas, M., & Oroian, M. (2020). Physicochemical properties of pectin from *Malus domestica* ‘Fälticeni’ apple

- pomace as affected by non-conventional extraction techniques. *Food Hydrocolloids*, 100, 105383. <https://doi.org/10.1016/j.foodhyd.2019.105383>
- Gao, J., Wu, M., Du, S., Zhang, H., Wang, S., & Ling, B. (2023a). Recent advances in food processing by radio frequency heating techniques: A review of equipment aspects. *Journal of Food Engineering*, 357, 111609. <https://doi.org/10.1016/j.jfoodeng.2023.111609>
- Gao, J., Zhang, H., Wang, S., & Ling, B. (2023b). Performance evaluation of an experimental radio frequency heating system designed for studying the solid-liquid extraction. *Innovative Food Science and Emerging Technologies*, 90, 103518. <https://doi.org/10.1016/j.ifset.2023.103518>
- Gerschenson, L., Fissore, E., Rojas, A., IdrovoEncalada, A., Zukowski, E., & Higuera Coelho, R. (2021). Pectins obtained by ultrasound from agroindustrial by-products. *Food Hydrocolloids*, 118, 106799. <https://doi.org/10.1016/j.foodhyd.2021.106799>
- Gharibzahedi, S., Smith, B., & Guo, Y. (2019a). Pectin extraction from common fig skin by different methods: The physicochemical, rheological, functional, and structural evaluations. *International Journal of Biological Macromolecules*, 136, 275–283. <https://doi.org/10.1016/j.ijbiomac.2019.06.040>
- Gharibzahedi, S., Smith, B., & Guo, Y. (2019b). Ultrasound-microwave assisted extraction of pectin from fig (*Ficus carica* L.) skin: Optimization, characterization and bioactivity. *Carbohydrate Polymers*, 222, 114992. <https://doi.org/10.1016/j.carbpol.2019.114992>
- Hosseini, S., Khodaiyan, F., Kazemi, M., & Najari, Z. (2019). Optimization and characterization of pectin extracted from sour orange peel by ultrasound assisted method. *International Journal of Biological Macromolecules*, 125, 621–629. <https://doi.org/10.1016/j.ijbiomac.2018.12.096>
- Hu, W., Chen, S., Wu, D., Zhu, K., & Ye, X. (2021). Manosonication assisted extraction and characterization of pectin from different citrus peel wastes. *Food Hydrocolloids*, 121, 106952. <https://doi.org/10.1016/j.foodhyd.2021.106952>
- Jamshidi, E., Behzad, F., Adabi, M., & Esnaashari, S. (2024). Edible iron-pectin nanoparticles: Preparation, physicochemical characterization and release study. *Food and Bioprocess Technology*, 17(3), 628–639. <https://doi.org/10.1007/s11947-023-03156-4>
- Kazemi, M., Khodaiyan, F., & Hosseini, S. (2019). Utilization of food processing wastes of eggplant as a high potential pectin source and characterization of extracted pectin. *Food Chemistry*, 294, 339–346. <https://doi.org/10.1016/j.foodchem.2019.05.063>
- Khedmat, L., Izadi, A., Mofid, V., & Mojtahedi, S. (2020). Recent advances in extracting pectin by single and combined ultrasound techniques: A review of techno-functional and bioactive health-promoting aspects. *Carbohydrate Polymers*, 229, 115474. <https://doi.org/10.1016/j.carbpol.2019.115474>
- Kumari, M., Singh, S., & Chauhan, A. (2023). A comparative study of the extraction of pectin from Kinnow (*Citrus reticulata*) peel using different techniques. *Food and Bioprocess Technology*, 16(10), 2272–2286. <https://doi.org/10.1007/s11947-023-03059-4>
- Lal, A., Prince, M., Kothakota, A., Pandiselvam, R., Thirumdas, R., Mahanti, N., & Sreeja, R. (2021). Pulsed electric field combined with microwave-assisted extraction of pectin polysaccharide from jackfruit waste. *Innovative Food Science and Emerging Technologies*, 74, 102844. <https://doi.org/10.1016/j.ifset.2021.102844>
- Li, X., Bi, J., Jin, X., Li, X., Wu, X., & Lyu, J. (2020). Characterization of water binding properties of apple pectin modified by instant controlled pressure drop drying (DIC) by LF-NMR and DSC methods. *Food and Bioprocess Technology*, 13(2), 265–274. <https://doi.org/10.1007/s11947-019-02387-8>
- Li, H., Wang, J., Wang, S., & Ling, B. (2022). Performance evaluation of the double screw conveyor in radio frequency systems: Heating uniformity and quality of granular foods. *Innovative Food Science and Emerging Technologies*, 77, 102990. <https://doi.org/10.1016/j.ifset.2022.102990>
- Liew, S., Ngoh, G., Yusoff, R., & Teoh, W. (2016). Sequential ultrasound-microwave assisted acid extraction (UMAE) of pectin from pomelo peels. *International Journal of Biological Macromolecules*, 93, 426–435. <https://doi.org/10.1016/j.ijbiomac.2016.08.065>
- Lin, Y., An, F., He, H., Geng, F., Song, H., & Huang, Q. (2021). Structural and rheological characterization of pectin from passion fruit (*Passiflora edulis* f. *flavicarpa*) peel extracted by high-speed shearing. *Food Hydrocolloids*, 114, 106555. <https://doi.org/10.1016/j.foodhyd.2020.106555>
- Ling, B., Ramaswamy, H., Lyng, J., Gao, J., & Wang, S. (2023). Roles of physical fields in the extraction of pectin from plant food wastes and byproducts: A systematic review. *Food Research International*, 164, 112343. <https://doi.org/10.1016/j.foodres.2022.112343>
- Liu, L., Guan, X., Jiao, Q., Xu, J., Li, R., Erdogdu, F., & Wang, S. (2023). Developing combined radio frequency with water bath treatments to improve gel properties of minced chicken breast. *Food and Bioprocess Technology*, 17(1), 138–153. <https://doi.org/10.1007/s11947-023-03127-9>
- Mahmood, N., Liu, Y., Saleemi, M., Munir, Z., Zhang, Y., & Saeed, R. (2023). Investigation of physicochemical and textural properties of brown rice by hot air assisted radio frequency drying. *Food and Bioprocess Technology*, 16(7), 1555–1569. <https://doi.org/10.1007/s11947-023-03001-8>
- Muñoz, I., de Sousa, D., Guardia, M., Rodriguez, C., Nunes, M., Oliveira, H., Cunha, S., Casal, S., Marques, A., & Cabado, A. (2022). Comparison of different technologies (Conventional thermal processing, radiofrequency heating and high-pressure processing) in combination with thermal solar energy for high quality and sustainable fish soup pasteurization. *Food and Bioprocess Technology*, 15(4), 795–805. <https://doi.org/10.1007/s11947-022-02782-8>
- Naik, M., Rawson, A., & Rangarajan, J. (2020). Radio frequency-assisted extraction of pectin from jackfruit (*Artocarpus heterophyllus*) peel and its characterization. *Journal of Food Process Engineering*, 43(6), e13389. <https://doi.org/10.1111/jfpe.13389>
- Panwar, D., Panesar, P. S., & Chopra, H. K. (2023). Ultrasound-assisted extraction of pectin from *Citrus limetta* peels: Optimization, characterization, and its comparison with commercial pectin. *Food Bioscience*, 51, 102231. <https://doi.org/10.1016/j.fbio.2022.102231>
- Rahmani, Z., Khodaiyan, F., Kazemi, M., & Sharifan, A. (2020). Optimization of microwave-assisted extraction and structural characterization of pectin from sweet lemon peel. *International Journal of Biological Macromolecules*, 147, 1107–1115. <https://doi.org/10.1016/j.ijbiomac.2019.10.079>
- Rodsamran, P., & Sothornvit, R. (2019). Microwave heating extraction of pectin from lime peel: Characterization and properties compared with the conventional heating method. *Food Chemistry*, 278, 364–372. <https://doi.org/10.1016/j.foodchem.2018.11.067>
- Sengar, A., Rawson, A., Muthiah, M., & Kalakandan, S. (2020). Comparison of different ultrasound assisted extraction techniques for pectin from tomato processing waste. *Ultrasonics Sonochemistry*, 61, 104812. <https://doi.org/10.1016/j.ultsonch.2019.104812>
- Su, D., Li, P., Quek, S., Huang, Z., Yuan, Y., Li, G., & Shan, Y. (2019). Efficient extraction and characterization of pectin from orange peel by a combined surfactant and microwave assisted process. *Food Chemistry*, 286, 1–7. <https://doi.org/10.1016/j.foodchem.2019.01.200>
- Tao, Y., Li, D., Siong Chai, W., Show, P., Yang, X., Manickam, S., Xie, G., & Han, Y. (2021). Comparison between airborne ultrasound and contact ultrasound to intensify air drying of blackberry: Heat

- and mass transfer simulation, energy consumption and quality evaluation. *Ultrasonics Sonochemistry*, 72, 105410. <https://doi.org/10.1016/j.ultsonch.2020.105410>
- Tao, Y., Wu, P., Dai, Y., Luo, X., Manickam, S., Li, D., Han, Y., & Show, P. (2022). Bridge between mass transfer behavior and properties of bubbles under two-stage ultrasound-assisted physorption of polyphenols using macroporous resin. *Chemical Engineering Journal*, 436, 135158. <https://doi.org/10.1016/j.cej.2022.135158>
- Thu Dao, T. A., Webb, H. K., & Malherbe, F. (2021). Optimization of pectin extraction from fruit peels by response surface method: Conventional versus microwave-assisted heating. *Food Hydrocolloids*, 113, 106475. <https://doi.org/10.1016/j.foodhyd.2020.106475>
- Tien, N., Le, N., Khoi, T., & Richel, A. (2022). Optimization of microwave-ultrasound-assisted extraction (MUAE) of pectin from dragon fruit peels using natural deep eutectic solvents (NADES). *Journal of Food Processing and Preservation*, 46(1), e16117. <https://doi.org/10.1111/jfpp.16117>
- Tocmo, R., Pena-Fronteras, J., Calumba, K. F., Mendoza, M., & Johnson, J. J. (2020). Valorization of pomelo (*Citrus grandis* Osbeck) peel: A review of current utilization, phytochemistry, bioactivities, and mechanisms of action. *Comprehensive Reviews in Food Science and Food Safety*, 19(4), 1969–2012. <https://doi.org/10.1111/1541-4337.12561>
- Tunç, M., & Odabaş, H. (2021). Single-step recovery of pectin and essential oil from lemon waste by ohmic heating assisted extraction/hydrodistillation: A multi-response optimization study. *Innovative Food Science and Emerging Technologies*, 74, 102850. <https://doi.org/10.1016/j.ifset.2021.102850>
- Wandee, Y., Uttapap, D., & Mischnick, P. (2019). Yield and structural composition of pomelo peel pectins extracted under acidic and alkaline conditions. *Food Hydrocolloids*, 87, 237–244. <https://doi.org/10.1016/j.foodhyd.2018.08.017>
- Wang, W., Ma, X., Xu, Y., Cao, Y., Jiang, Z., Ding, T., Ye, X., & Liu, D. (2015). Ultrasound-assisted heating extraction of pectin from grapefruit peel: Optimization and comparison with the conventional method. *Food Chemistry*, 178, 106–114. <https://doi.org/10.1016/j.foodchem.2015.01.080>
- Wang, W., Ma, X., Jiang, P., Hu, L., Zhi, Z., Chen, J., Ding, T., Ye, X., & Liu, D. (2016). Characterization of pectin from grapefruit peel: A comparison of ultrasound-assisted and conventional heating extractions. *Food Hydrocolloids*, 61, 730–739. <https://doi.org/10.1016/j.foodhyd.2016.06.019>
- Wang, W., Wu, X., Chantapakul, T., Wang, D., Zhang, S., Ma, X., Ding, T., Ye, X., & Liu, D. (2017). Acoustic cavitation assisted extraction of pectin from waste grapefruit peels: A green two-stage approach and its general mechanism. *Food Research International*, 102, 101–110. <https://doi.org/10.1016/j.foodres.2017.09.087>
- Wang, C., Qiu, W., Chen, T., & Yan, J. (2021). Effects of structural and conformational characteristics of citrus pectin on its functional properties. *Food Chemistry*, 339, 128064. <https://doi.org/10.1016/j.foodchem.2020.128064>
- Xiao, L., Ye, F., Zhou, Y., & Zhao, G. (2021). Utilization of pomelo peels to manufacture value-added products: A review. *Food Chemistry*, 351, 129247. <https://doi.org/10.1016/j.foodchem.2021.129247>
- Yang, J., Mu, T., & Ma, M. (2019). Optimization of ultrasound-microwave assisted acid extraction of pectin from potato pulp by response surface methodology and its characterization. *Food Chemistry*, 289, 351–359. <https://doi.org/10.1016/j.foodchem.2019.03.027>
- Yang, N., Jin, Y., Zhou, Y., & Zhou, X. (2024). Physicochemical characterization of pectin extracted from mandarin peels using novel electromagnetic heat. *International Journal of Biological Macromolecules*, 262, 130212. <https://doi.org/10.1016/j.ijbiomac.2024.130212>
- Zheng, J., Li, H., Wang, D., Li, R., Wang, S., & Ling, B. (2021). Radio frequency assisted extraction of pectin from apple pomace: Process optimization and comparison with microwave and conventional methods. *Food Hydrocolloids*, 121, 107031. <https://doi.org/10.1016/j.foodhyd.2021.107031>

**Publisher's Note** Springer Nature remains neutral with regard to jurisdictional claims in published maps and institutional affiliations.

Springer Nature or its licensor (e.g. a society or other partner) holds exclusive rights to this article under a publishing agreement with the author(s) or other rightsholder(s); author self-archiving of the accepted manuscript version of this article is solely governed by the terms of such publishing agreement and applicable law.